

Thermal ageing of nanostructured tetragonal zirconia ceramics: Characterization of interfaces

R.A. Rocha^{a,b,*}, E.N.S. Muccillo^b, L. Dessemond^a, E. Djurado^a

^a *Laboratoire d'Electrochimie et de Physico-chimie des Matériaux et des Interfaces, Grenoble INP/UJF, CNRS, UMR 5631, 1130 Rue de la Piscine, BP 75, 38402 Saint-Martin d'Hères, France*

^b *IPEN, CCTM/CMDMC, Rua do Matão, Travessa R 400, Cidade Universitária, 05508-000 São Paulo, SP, Brazil*

Available online 31 May 2009

Abstract

This paper reports the preparation of nanometric powders of 3.5 mol% Y₂O₃-doped ZrO₂, with controlled microstructure, by the spray pyrolysis process, assisted by ultrasonic atomizer, at relatively low temperature. As-prepared powders were found crystalline and consisted of dense and chemically homogeneous spherical particles. Conventional sintering at 1500 °C for 2 h in air yields dense ceramics of 83 nm of average grain size. The electrical properties of electrode/electrolyte interface were determined by impedance spectroscopy measurements before, during and after thermal ageing for 2000 h at 700 °C in dry air. The effect of thermal ageing on the electrical responses of the ceramic and interfaces with platinum electrodes was investigated.

© 2009 Elsevier Ltd. All rights reserved.

Keywords: C. Ionic conductivity; D. ZrO₂; Impedance spectroscopy; Nanostructured powders-chemical preparation; Thermal ageing

1. Introduction

Ytria-stabilized zirconia (YSZ) is the common electrolyte in solid oxide fuel cells (SOFCs).¹ However, small grain sizes (<1 μm) required for high strength gives rise to a material with a large total grain boundary surface area,² which can have a detrimental effect on the electrolyte conductivity. In nanocrystalline YSZ, the specific grain boundary conductivity, used to quantify the microstructure effects on the additional blocking effect of charge carriers,³ was reported to be 1–2 orders of magnitude higher than that of coarse-grained YSZ making this a promising electrolyte material for solid state electrochemical devices.^{4–7} Tetragonal zirconia polycrystalline (TZP) ceramics are also a candidate electrolyte for oxygen sensors and fuel cells because of excellent thermo-mechanical properties⁸ and ionic conductivity, comparable or better than that of YSZ.⁹ However, these materials can undergo a phase transformation from tetragonal to monoclinic when annealed in a relatively low temperature range.¹⁰ This yields a degradation of both mechanical properties

and conductivity.¹¹ High performances and long term stability of electrical properties are required for practical use of SOFCs.¹² However, it is well known that the conductivity of zirconia-based ceramics decreases during ageing at temperatures above 800 °C. Many studies have been devoted to YSZ^{12–18} although investigations of the ageing of TZP are scarce,¹⁹ especially for grain sizes lower than 300 nm.

In this study, the microstructure and conductivity of nanostructured tetragonal zirconia were compared. Impedance spectroscopy, a powerful tool to investigate the electrical behaviour of polycrystalline zirconia,^{20,21} was used to monitor the evolution of the response of symmetrical cells in conditions close to those of a SOFC.

2. Experimental

ZrO₂:3.5 mol% Y₂O₃ (Y-TZP) powders were prepared by a spray pyrolysis technique. The precursor solutions were prepared by dissolution of ZrO(NO₃)₂·xH₂O (Fluka) and Y(NO₃)₃·4H₂O (Aldrich, 99.999%) in distilled water. The concentration of final solution was fixed at 2.5 × 10⁻² mol L⁻¹. This solution was atomized by a 1.7 MHz frequency ultrasonic generator, yielding an aerosol, which was carried through a three-zone tubular furnace by a N₂ + O₂ mixture, with a flow rate of 6 L min⁻¹. The temperature of the tubular furnace was

* Corresponding author at: Rua do Matão, Travessa R 400, Cidade Universitária, 05508-000, São Paulo, SP, Brazil. Tel.: +55 11 3133 9232; fax: +55 11 3133 9276.

E-mail address: rarochoa@ipen.br (R.A. Rocha).

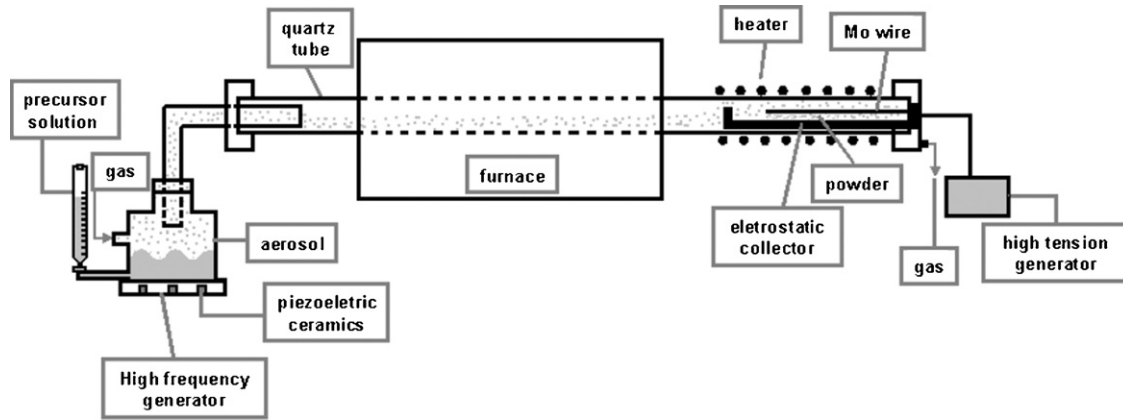


Fig. 1. Experimental system for the spray pyrolysis synthesis.

fixed at 600 °C. The experimental system is shown in Fig. 1. $\text{ZrO}_2:3.5 \text{ mol\% Y}_2\text{O}_3$ pellets were obtained after uniaxial and isostatic pressing and sintered in air at 1500 °C for 2 h.

Powder and ceramic samples were characterized by X-ray diffraction (XRD) at room temperature (Siemens D500), using $\text{Cu K}\alpha$ radiation, in the $20^\circ < 2\theta < 80^\circ$ range, with 0.04° (2θ) step size and 8 s counting time, to determine the crystalline phases and the average crystallite size, using the Scherrer equation. Crystalline phases were also identified by Raman spectroscopy (Jobin Yvon T64000 or Dilor XY), using the excitation line of an argon ion laser ($\lambda = 514.5 \text{ nm}$). Relative density was measured from dimensions and weight of the pellets. Fracture surface of dense pellets were observed by field emission gun scanning electron microscopy (FEG-SEM) (Zeiss Ultra 55) before and after isothermal ageing.

Impedance spectroscopy measurements were performed on symmetrical cells. Platinum paste was deposited on both sides of pellets and heated at 700 °C for 2 h in air. Platinum grids were used as current collectors. Electrical measurements in the low frequency range (10^4 to 10^{-2} Hz) were obtained by using a Solartron 1280B potentiostat/frequency response analyzer. For higher frequencies (1.3×10^7 to 5 Hz), a Hewlett-Packard impedancemeter (4192A LF) was used. The whole impedance of investigated cell was determined under zero DC conditions during ageing at 700 °C for 2000 h in dry air. The electrical properties of zirconia pellets were also recorded at 400 °C before and after isothermal ageing to distinguish between contributions of grains and grain boundaries to the resistivity. The magnitude of the ac signal was 20 and 200 mV for low frequency measurements and high frequency ones, respectively. Impedance diagrams of ceramic pellets are normalized by a unit geometrical factor and characteristics of platinum/zirconia interfaces are normalized by the electrodes area. Numbers on experimental diagrams indicate the logarithm of the ac measuring frequency.

3. Results and discussion

Spray pyrolysis technique provides nanocrystalline powders of $\text{ZrO}_2:\text{Y}_2\text{O}_3$ of high purity at relatively low temperature. No trace of amorphous phase was detected. The diffraction peaks can be indexed in tetragonal symmetry, according to ICDD

file 01-070-4426 (Fig. 2). In the Y-TZP diffraction pattern, the absence of splitting in two different lines, characteristic of a tetragonal structure, may be due to the small crystallite size or to the structural c/a ratio near 1 (t'' structure).²² By applying Scherrer formula, the crystallite size in as-synthesized powders was found to be 5.8 nm. After sintering at 1500 °C for 2 h in air, a 83 nm average grain size was determined. In contradiction to literature data,²³ a limited grain growth was observed. This is likely to be due to the presence of a crystallized envelope containing aggregated primary crystallites of about 80 nm and also because of the good purity of investigated materials.²⁴

The as-prepared powder has spherical, homogeneous and dense particles, with a narrow particle size distribution (Fig. 3). The sintered density is about 97% of theoretical one and the fracture surface is typical of a dense material. If one refers to Fig. 3, the average grain size determined by XRD appears to be smaller than the observed ones. It can be thus inferred that these particles are consisted of aggregates of small crystallites corresponding to single crystalline volumes.

Raman spectroscopy is sensitive both to oxygen displacements due to the large polarizability and to the intermediate range order without the long-range periodicity.²² As shown in Fig. 4, Raman spectra obtained at room temperature confirmed the tetragonal phase. Indeed, the Raman frequencies of vibration at 641, 640, 460, 319, and 264 cm^{-1} are, respectively,

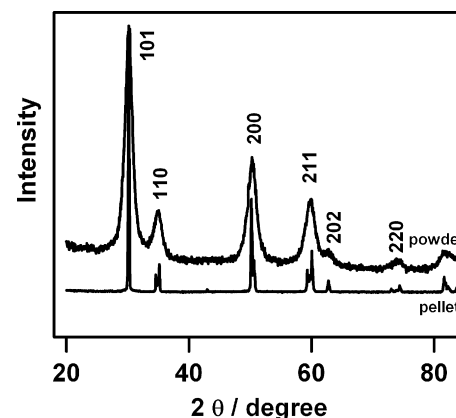


Fig. 2. X-ray diffraction patterns of 3.5 mol% Y_2O_3 -doped ZrO_2 .

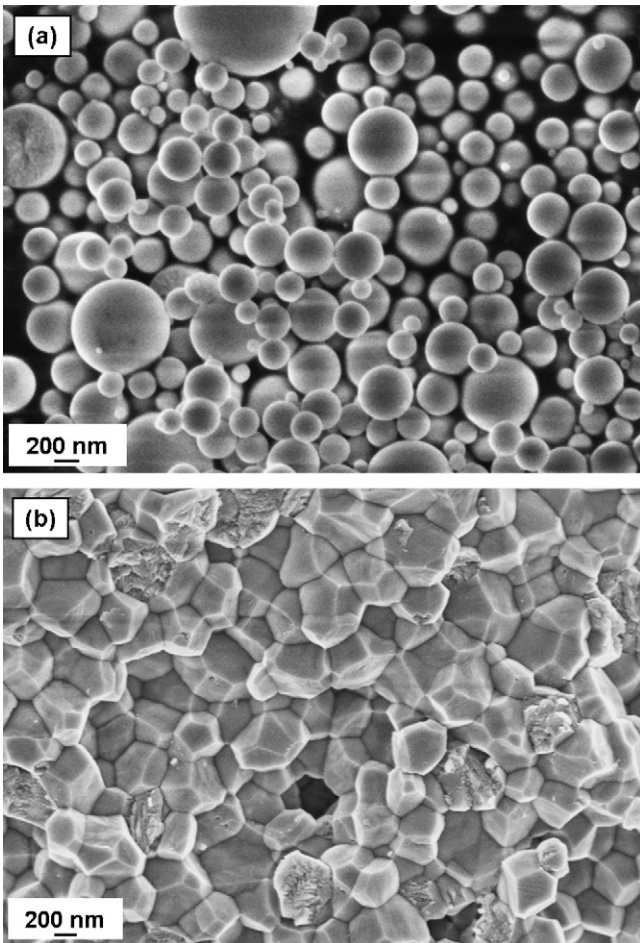


Fig. 3. Scanning electron microscopy images of (a) as-prepared powder and (b) fracture surface of a sintered pellet.

associated to E_g , A_{1g} , E_g , B_{1g} , and E_g symmetry modes of tetragonal zirconia. In the absence of additional peaks corresponding to the monoclinic phase²⁵ and without any variation of the Raman spectra, one can conclude that no structural modification occurred in the chosen ageing conditions. No evident grain growth was observed after ageing, as shown in Fig. 5, indi-

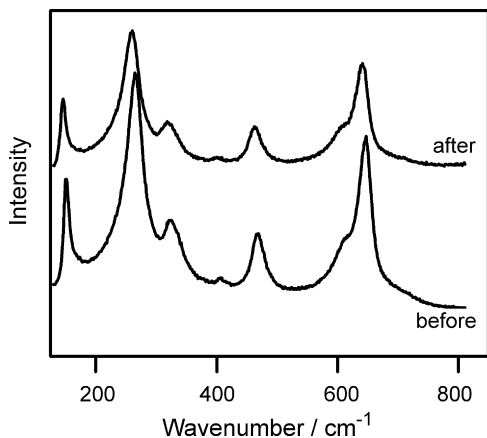


Fig. 4. Raman spectra of Y-TZP samples before and after ageing at 700 °C/2000 h in dry air.

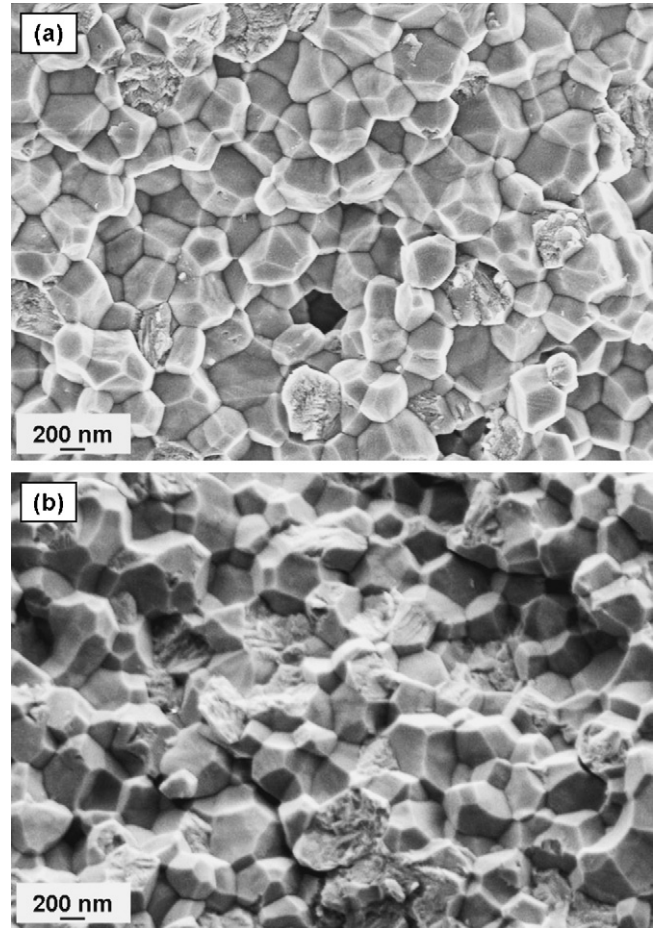


Fig. 5. Scanning electron microscopy images of fracture surface of dense Y-TZP sample (a) before and (b) after ageing at 700 °C for 2000 h in dry air.

ating that the grain boundaries density do not vary significantly during the high temperature treatment.

Concerning thermal ageing at 700 °C for 2000 h in dry air, impedance spectroscopy measurements were carried out to evaluate the electrical behaviour of Y-TZP dense samples.

Impedance diagrams recorded at 400 °C before and after ageing are composed of two fairly well separated semicircles in the Nyquist plane (Fig. 6). The high frequency semicircle represents the specific contribution of zirconia grains and the intermediate frequency one is related to the blocking effect due to internal interfaces. The low frequency contribution is characteristic of

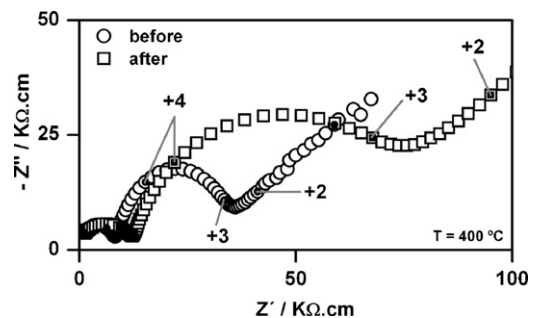


Fig. 6. Impedance spectroscopy diagrams recorded at 400 °C, before and after ageing at 700 °C for 2000 h in dry air.

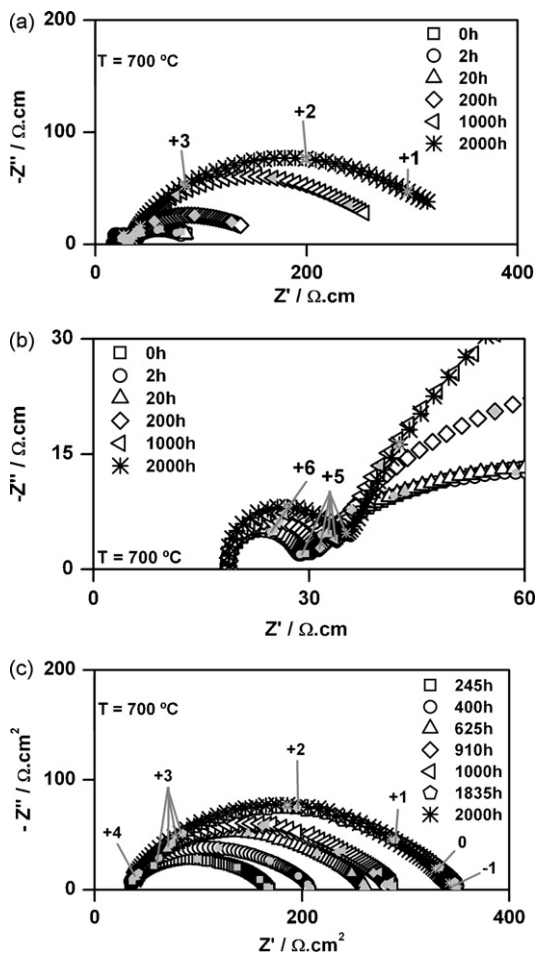


Fig. 7. Impedance spectroscopy diagrams recorded during ageing at 700 °C: (a) high frequencies response, (b) electrolyte contribution and (c) low frequencies electrode characteristic.

the platinum/zirconia interfaces. The magnitude of the electrode characteristic was deduced from impedance measurements performed in the lowest frequencies range during ageing. It is worth noting that the good separation between the electrode characteristic and the zirconia response suggests intimate contacts at the platinum/zirconia interfaces.

At 700 °C, only the total electrolyte resistivity $\rho_t = \rho_b + \rho_{bl}$ (ρ_b and ρ_{bl} represent the bulk and the blocking resistivities, respectively) and the normalized electrode resistance R_{el} were determined accurately because of the inductive effect of platinum wires in the measuring cell (Fig. 7). The electrolyte resistivity is an increasing function of ageing time, in agreement with literature data on zirconia-based ceramics.^{15–18} For Y-TZP pellets also prepared by spray pyrolysis, with 60 nm of average grain size,²⁰ an increase of only 5% of ρ_t was observed after 1000 h at 700 °C. The recorded results are not in contradiction since present measurements were performed over a period of 2000 h and conductivity is a decreasing function of ageing time.¹² Nevertheless, no changes were observed in both shape and frequency distribution of the zirconia impedance diagrams for the whole ageing period. One can thus expect that no phase transition occurred within the sample,^{26,27} in agreement with Raman characterizations (Fig. 4). At 400 °C, ρ_b and ρ_{bl} increase

by a factor of 1.5 and by a factor of 2.3, respectively, after ageing (Fig. 6). An increase of the bulk resistivity has been observed in some YSZ samples after isothermal treatments performed at temperatures above 700 °C. This was related to the formation of an additional phase¹⁸ or to short range ordering of atomic species.²⁸ At this stage, one can only infer that the increase of ρ_b does not originate from any significant structural changes.

Since the grain size remains nearly constant, and without any phase transition, the main increase of the blocking effect is rather surprising. But, one must keep in mind that the magnitude of this contribution depends on thermal history. Indeed, a large variation of the additional blocking effect was evidenced for 2.5 mol% Y₂O₃-doped nanostructured tetragonal zirconia by quenching from high temperatures in air.²⁹ This was related to a modified magnitude of dopant segregation at grain boundaries which can affect the recorded blocking resistivity.³⁰

In agreement with previously published data,³¹ the electrode resistance shows the strongest degradation versus ageing time (Fig. 7). Without any significant change of the frequency distribution, the recorded increase of R_{el} cannot be thus related to an alteration of the electrode reaction mechanism³² or to the formation of monoclinic phase.³³ The recorded increasing indicates a reduction of current pathways at the zirconia/platinum interfaces.³⁴ Nevertheless, the microstructure of the platinum electrodes is likely to be stable in the chosen experimental conditions. Thus, the decreasing electrode reaction rate may originate from chemical modifications at platinum/zirconia interfaces. An HR-TEM study is in progress to provide experimental data for grain boundaries and more reliable information on grain size before and after ageing.

4. Conclusions

Spray pyrolysis is a technique that can provide nanocrystalline powders of single phase tetragonal zirconia at relatively low temperature. Both electrolyte resistivity and electrode resistance are increasing functions of ageing time at 700 °C in dry air. Impedance measurements performed at lower temperatures enable to quantify the influence on both electrical contributions of the material. The main degradations seem to be related to chemical modifications at electrode/electrolyte interfaces and in the vicinity of grain boundaries. Y-TZP appears to be promising for a long life intermediate temperature solid oxide fuel cell.

Acknowledgement

The authors are grateful to acknowledge CNPq – Brazil (200201/2005-8) for the post doctorate scholarship of R.A. Rocha in LEPMI (France).

References

1. Badwal, S. P. S., In *Proceedings of 1st European Solid Oxide Fuel Cells Forum, Switzerland*, ed. U. Bossel, 1994, pp. 399–414.
2. Badwal, S. P. S. and Drennan, J., The effect of thermal history on the grain boundary resistivity of Y-TZP materials. *Solid State Ionics*, 1998, **28–30**, 1451–1455.

3. Aoki, M., Chiang, Y.-M., Kosacki, I., Lee, L. J.-R., Tuller, H. and Liu, Y., Solute segregation and grain-boundary impedance in high-purity stabilized zirconia. *Journal of the American Ceramic Society*, 1996, **79**, 1169–1180.
4. Shukla, S., Seal, S., Vij, R. and Bandyopadhyay, S., Reduced activation energy for grain growth in nanocrystalline yttria-stabilized zirconia. *Nano Letters*, 2003, **3**(3), 397–401.
5. Mondal, P., Klein, A., Jaegermann, W. and Hahn, H., Enhanced specific grain boundary conductivity in nanocrystalline Y_2O_3 -stabilized zirconia. *Solid State Ionics*, 1999, **118**, 331–339.
6. Choen, K.-W., Chen, J. and Xu, R., Metal–organic vapor deposition of YSZ electrolyte layers for solid oxide fuel cell applications. *Thin Solid Films*, 1997, **304**, 106–112.
7. Liaw, B. Y. and Weppner, W., Low temperature limiting-current oxygen sensors based on tetragonal zirconia polycrystals. *Journal of the Electrochemical Society*, 1991, **138**, 2478–2483.
8. Rühle, M., Claussen, N. and Heuer, A. H., Microstructural studies of Y_2O_3 containing tetragonal ZrO_2 polycrystals (Y-TZP). *Advances in Ceramics*, 1984, **12**, 352–370.
9. Badwal, S. P. S., Effect of dopant concentration on the grain boundary and volume resistivity of yttria-zirconia. *Journal of Materials Science Letters*, 1987, **6**, 1419–1421.
10. Lawson, S., Environmental degradation of zirconia ceramics. *Journal of the European Ceramic Society*, 1995, **15**, 485–502.
11. Kim, D.-J., Jung, H.-J., Jang, J.-W. and Lee, H.-L., Fracture toughness, ionic conductivity, and low-temperature phase stability of tetragonal zirconia codoped with yttria and niobium oxide. *Journal of the American Society*, 1998, **81**, 2309–2314.
12. Vlasov, A. N. and Perfiliev, M. V., Ageing of ZrO_2 -based solid electrolytes. *Solid State Ionics*, 1987, **25**, 245–253.
13. Gibson, R., Dransfield, G. P. and Irvine, J. T. S., Influence of yttria concentration upon electrical properties and susceptibility to ageing of yttria-stabilised zirconias. *Journal of the European Ceramic Society*, 1998, **18**, 661–667.
14. Nomura, K., Mizutani, Y., Kawai, M., Nakamura, Y. and Yamamoto, O., Aging and Raman scattering study of scandia and yttria doped zirconia. *Solid State Ionics*, 2000, **132**, 235–239.
15. Kondon, J., Shiota, H., Kikuchi, S., Tomii, Y., Ito, Y. and Kawachi, K., Changes in aging behavior and defect structure of Y_2O_3 fully stabilized ZrO_2 by In_2O_3 doping. *Journal of the Electrochemical Society*, 2002, **149**, J59–J72.
16. Hattori, M., Takeda, Y., Sakaki, Y., Nakanishi, A., Ohara, S., Mukai, K., Lee, J.-H. and Fukui, T., Effect of aging on conductivity of yttria stabilized zirconia. *Journal of Power Sources*, 2004, **126**, 23–27.
17. Haering, C., Roosen, A. and Schichl, H., Degradation of the electrical conductivity in stabilised zirconia systems. Part I. Yttria-stabilised zirconia. *Solid State Ionics*, 2005, **176**, 253–259.
18. Butz, B., Kruse, P., Störmer, H., Gerthsen, D., Müller, A., Weber, A. and Ivers-Tiffée, E., Correlation between microstructure and degradation in conductivity for cubic Y_2O_3 -doped ZrO_2 . *Solid State Ionics*, 2005, **177**, 3275–3284.
19. Kondon, J., Kawashima, T., Kikuchi, S., Tomii, Y. and Ito, Y., Effect of aging on yttria-stabilized zirconias. *Journal of the Electrochemical Society*, 1998, **145**, 1527–1536.
20. Boulc'h, F., Dessemond, L. and Djurado, E., Delay of tetragonal-to-monoclinic transition in water vapour due to nanostructural effect. *Journal of the European Ceramic Society*, 2004, **24**, 1181–1185.
21. Muccillo, E. N. S. and Kleitz, M., Impedance spectroscopy of Mg-partially stabilized zirconia and cubic phase decomposition. *Journal of the European Ceramic Society*, 1996, **16**, 453–465.
22. Yashima, M., Ohtake, K., Kakihana, M., Arashi, H. and Yoshimura, M., Determination of tetragonal-cubic phase boundary of $Zr_{1-x}R_xO_{2-x/2}$ ($R = Nd, Sm, Y, Er$ and Yb) by Raman Scattering. *Journal of Physics and Chemistry of Solids*, 1996, **57**, 17–24.
23. Mayo, M. J., Processing of nanocrystalline ceramics from ultrafine particles. *International Materials Reviews*, 1996, **41**, 85–115.
24. Boulc'h, F. and Djurado, E., Structural changes of rare-earth-doped, nanostructured zirconia solid solution. *Solid State Ionics*, 2003, **157**, 335–340.
25. Kim, B.-K., Hahn, J.-W. and Han, K. R., Quantitative analysis in tetragonal-rich tetragonal/monoclinic two phase zirconia by Raman spectroscopy. *Journal of Materials Science Letters*, 1997, **16**, 669–671.
26. Kleitz, M. and Steil, M. C., Microstructure blocking effects versus effective medium theories in YSZ. *Journal of the European Ceramic Society*, 1997, **17**, 819–829.
27. Butler, E. P. and Bonanos, N., The characterization of ZrO_2 engineering ceramics by a.c. impedance spectroscopy. *Materials Science and Engineering*, 1985, **71**, 49–56.
28. Balakrishnan, N., Takeuchi, T., Nomura, K., Kageyama, H. and Takeda, Y., Aging effect of 8 mol% Y_2O_3 YSZ with different microstructures. *Journal of the Electrochemical Society*, 2004, **151**, A1286–A1291.
29. Boulc'h, F., PhD Thesis. Institut National Polytechnique de Grenoble, Grenoble, France; 2002.
30. Guo, X. and Maier, J., Grain boundary blocking effect in zirconia: a Schottky barrier analysis. *Journal of the Electrochemical Society*, 2001, **148**, E121–E126.
31. Djurado, E., Boulc'h, F., Dessemond, L., Rosman, N. and Mermoux, M., Study on aging of tetragonal zirconia by coupling impedance and Raman spectroscopies in water vapour atmosphere. *Journal of the Electrochemical Society*, 2004, **151**, A774–A780.
32. Mitterdorfer, A. and Gauckler, L. J., $La_2Zr_2O_7$ formation and oxygen reduction kinetics of the $La_{0.85}Sr_{0.15}Mn_yO_{3+O_2(g)}$ YSZ system. *Solid State Ionics*, 1998, **111**, 185–218.
33. Badwal, S. P. S. and Nardella, N., Formation of monoclinic zirconia at the anodic face of tetragonal zirconia polycrystalline solid electrolytes. *Applied Physics A*, 1989, **49**, 13–24.
34. Fleig, J. and Maier, J., The Influence of current constriction on the impedance of polarizable electrodes. *Journal of the Electrochemical Society*, 1997, **144**, L302–L305.